Narrow-azimuth migration of marine streamer data

Biondo Biondi, Stanford University

SUMMARY

I introduce a new migration method that overcomes the limitations of common-azimuth migration while retaining its computational efficiency for imaging marine streamer data. The method is based on source-receiver downward-continuation of the prestack data with a narrow range of cross-line offsets. To minimize the width of the cross-line offset range, while assuring that all the recorded events are correctly propagated, I define an "optimal" range of cross-line offset dips. To remove the effects of the boundary artifacts I apply a coplanarity condition on the prestack image. This process removes from the image cube the events that are not correctly focused at zero offset. Tests of the proposed method with the SEG-EAGE salt dataset show substantial image improvements in particularly difficult areas of the model and thus confirm the theoretical advantages of the new method over common azimuth migration

INTRODUCTION

Common-azimuth (Biondi and Palacharla, 1996) is an attractive alternative to shot-profile migration for wave-equation 3-D prestack migration. For 3-D marine streamer data, it is computationally more efficient than shot-profile migration and thus it has been implemented in different migration algorithms (Jin et al., 2002) and applied to several datasets (Fliedner et al., 2002; Le Rousseau et al., 2002). In addition to the computational efficiency, common-azimuth migration has the substantial advantage of enabling migration velocity analysis (Clapp and Biondi, 2000; Liu et al., 2001) by generating high-quality Angle-Domain Common Image Gathers (ADCIG) (Prucha et al., 1999) without additional computations. However, in presence of arbitrary velocity functions, common-azimuth migration is not exact. In this paper, we propose a method for generalizing common-azimuth migration that is accurate in presence of arbitrary velocity variations but retains its computational advantages with respect to shot-profile migration.

Common-azimuth migration is based on the principles of source-receiver (survey-sinking) migration (Claerbout, 1985). Source-receiver migration is theoretically equivalent to shot-profile migration based on downward continuation (Wapenaar and Berkhout, 1987; Biondi, 2002) (notice, not shot-profile migration based on time extrapolation), and thus the proposed generalization of common-azimuth migration has the potential to produce as high-quality images as the more computationally demanding shot-profile migration.

At the basis of common-azimuth computational efficiency is the exploitation of the narrow azimuthal range of typical marine data acquired by towed streamers. This is made possible by a crucial characteristics of source-receiver migration: during source-receiver downward continuation the offset range shrinks with depth. In most practical situations the offset range shrinks monotonically with depth, but this property is not guaranteed in arbitrarily heterogeneous media. At the limit, the cross-line offset can be assumed to be zero and all recorded events can be propagated with the same azimuth (e.g. common azimuth) at every depth level. The assumption of no cross-line offset provides the computational efficiency of common-azimuth migration, but also causes its accuracy limitations. In this paper I remove this assumption by downward continuing the data on a narrow, but finite, cross-line offset range. To achieve computational efficiency, the cross-line offset range must be as narrow as possible and still "capture" all the useful propagation paths and avoid boundary artifacts. I accomplish this goal by introducing two complementary procedures: 1) definition of an "optimal" range of cross-line offset dips for the downward continuation, and 2) application of a *coplanarity condition* on the prestack image that enhances the events that are well focused at the imaging point (zero offset). The next two sections introduce these two new concepts.

NARROW-AZIMUTH DOWNWARD CONTINUATION

To define the "optimal" range of cross-line offset dips for the downward continuation I exploit the information provided by the common-azimuth equation to define a range of cross-line offset wavenumbers. The common-azimuth equation provides the cross-line offset wavenumber k_{y_h} as a function of the other wavenumbers in the data when the data are propagated along a constant azimuth (Biondi and Palacharla, 1996). In the frequency-wavenumber domain the common-azimuth relationship is:

$$\widehat{k_{y_h}} = k_{y_m} \frac{\sqrt{\frac{\omega^2}{v^2(\mathbf{g},z)} - \frac{1}{4}\left(k_{x_m}+k_{x_h}\right)^2} - \sqrt{\frac{\omega^2}{v^2(\mathbf{s},z)} - \frac{1}{4}\left(k_{x_m}-k_{x_h}\right)^2}}{\sqrt{\frac{\omega^2}{v^2(\mathbf{g},z)} - \frac{1}{4}\left(k_{x_m}+k_{x_h}\right)^2} + \sqrt{\frac{\omega^2}{v^2(\mathbf{s},z)} - \frac{1}{4}\left(k_{x_m}-k_{x_h}\right)^2}}. \tag{1}$$

where ω is the temporal frequency, k_{x_m} and k_{y_m} are the midpoint wavenumbers, k_{x_h} is the offset wavenumbers, and $v(\mathbf{s},z)$ and $v(\mathbf{s},z)$ are the local velocities. Ideally we would like to define a range of k_{y_h} that is varying with depth, as a function of the local velocities. However, that may lead to complex implementation, and I chose a simpler solution. I define a range of k_{y_h} by setting a minimum velocity $v_{\min}$ and a maximum velocity $v_{\max}$, and define

$$k_{y_h}^{\min} = k_{y_m} \frac{\sqrt{\frac{\omega^2}{v_{\min}^2} - \frac{1}{4}\left(k_{x_m}+k_{x_h}\right)^2} - \sqrt{\frac{\omega^2}{v_{\min}^2} - \frac{1}{4}\left(k_{x_m}-k_{x_h}\right)^2}}{\sqrt{\frac{\omega^2}{v_{\min}^2} - \frac{1}{4}\left(k_{x_m}+k_{x_h}\right)^2} + \sqrt{\frac{\omega^2}{v_{\min}^2} - \frac{1}{4}\left(k_{x_m}-k_{x_h}\right)^2}}. \tag{2}$$

and

$$k_{y_h}^{\max} = k_{y_m} \frac{\sqrt{\frac{\omega^2}{v_{\max}^2} - \frac{1}{4}\left(k_{x_m}+k_{x_h}\right)^2} - \sqrt{\frac{\omega^2}{v_{\max}^2} - \frac{1}{4}\left(k_{x_m}-k_{x_h}\right)^2}}{\sqrt{\frac{\omega^2}{v_{\max}^2} - \frac{1}{4}\left(k_{x_m}+k_{x_h}\right)^2} + \sqrt{\frac{\omega^2}{v_{\max}^2} - \frac{1}{4}\left(k_{x_m}-k_{x_h}\right)^2}}. \tag{3}$$

The central point of the k_{y_h} range is then defined as a function of $k_{y_h}^{\min}$ and $k_{y_h}^{\max}$ as

$$\overline{k_{y_h}} = \frac{k_{y_h}^{\max} + k_{y_h}^{\min}}{2}, \tag{4}$$

and the range as

$$\overline{k_{y_h}} - \left(\frac{N_{y_h}}{2} - 1\right) dk_{y_h} \le k_{y_h} \le \overline{k_{y_h}} + \frac{N_{y_h}}{2} dk_{y_h}, \tag{5}$$

where N_{y_h} is the number of cross-line offsets and dk_{y_h} is the sampling in k_{y_h}. The cross-line-offset wavenumber sampling dk_{y_h} is the constant value

$$dk_{y_h 1} = \frac{2\pi}{N_{y_h}\Delta y_h}. \tag{6}$$

Migration results

To verify the accuracy of the narrow-azimuth downward continuation method I migrated a synthetic data set. The reflectivity field

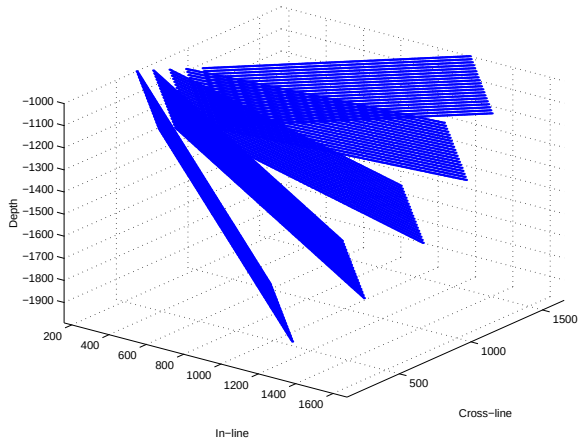

Figure 1: Geometry of the set of slanted planes, dipping at 0°, 15°, 30°, 45° and 60° toward increasing x and y, at 45° with respect to the in-line direction.

consists of a set of five dipping planes, from zero dip to 60 degrees dip. The azimuth of the planes is 45 degrees with respect to the direction of the acquisition. This reflection geometry (i.e. dipping reflectors oriented at 45 degrees with respect to the acquisition direction) is known to be the most challenging for common-azimuth migration. The velocity was $V(z) = 1.5 + .5z$ km/s, which corresponds to the upper limit among the typical gradients found in the Gulf of Mexico. The maximum source-receiver offset was 3 km. Figure 1 shows the geometry of the reflectors.

Figure 2 shows a subset of the image cube obtained by common-azimuth migration. The front face of the cube displayed in the figure is an in-line section through the stack. The other two faces are sections through the prestack image as a function of the offset ray parameter p_{x_h}. The three events in the ADCIG (right panel) correspond to the planes dipping at 30, 45 and 60 degrees. Notice that the events are almost perfectly flat as a function of the offset ray parameter p_{x_h}, except for the reflections from the 60-degrees plane with large offset ray parameters (i.e. large reflection angle). This slight smiling in the ADCIG is caused by the common-azimuth approximation.

The small error visible in the common-azimuth migration can be completely corrected by using full source-receiver migration. Figure 3 shows an ADCIG extracted at the same location as the ADCIG shown in Figure 2, but from the migrated image obtained by a full source-receiver migration. For these data, 16 cross-line offset were necessary to obtain an accurate image when using full source-receiver migration. In contrast, only 4 cross-line offsets are necessary to obtain an accurate image when using the narrow-azimuth downward continuation described in this section. Figure 4 shows an ADCIG extracted at the same location as the ADCIG shown in Figure 2, but from the migrated image obtained by narrow-azimuth migration with $N_{y_h} = 4$.

COPLANARITY CONDITION

As it can be observed in both Figure 3 and Figure 4, the image created by source-receiver downward continuation on a narrow cross-line offset range can be affected by strong artifacts caused by boundary effects. Effective absorbing boundary conditions require the addition of several grid points, and consequently a substantial increase in the computational cost. Fortunately, the boundary artifacts can be effectively removed by applying a post-processing filter on the prestack image that preserves only the events for which the source and receiver rays are coplanar at the imaging point. This condition must be fulfilled by all the events that are correctly focused at zero offset because two lines passing through the same point are coplanar. The *coplanarity condition* can be easily applied on the prestack image after transformation into the Fourier domain, possibly at the same time that ADCIGs are computed using a 3-D generalization of the method described by Sava and Fomel (2003), as presented in Biondi et al. (2003).

The coplanarity condition can be derived by simple geometric considerations starting from the common-azimuth condition expressed in equation (1). As for the common-azimuth condition, the coplanarity condition can be expressed as a relationship that links the cross-line offset wavenumber k_{y_h} to the other wavenumbers in the image. For events with azimuth aligned along the in-line direction (x_m in my notation), the expression of the coplanarity condition is:

$$k_{y_h} = \frac{k_{y_m} k_{x_m} k_{x_h}}{k_z \sqrt{k_z^2 + k_{y_m}^2}}. \tag{7}$$

The condition expressed in equation (7) can be easily generalized to be valid for an arbitrary azimuthal direction ϕ. The wavenumber axes are rotated by ϕ in both the midpoint wavenumber plane (k_{x_m}, k_{y_m}) and the offset wavenumber plane (k_{x_h}, k_{y_h}).

The final image can be obtained by stacking all the images obtained for a range of ϕ. This range is typically fairly narrow (± 15 degrees) because of the narrow-azimuth nature of streamer data.

SEG-EAGE salt data set migration results

The improvement in image quality achieved by applying source-receiver migration on a narrow range of cross-line offsets in conjunction with the coplanarity condition is demonstrated in the following results obtained from the SEG-EAGE salt data set. Figure 5a shows the in-line section of the velocity model taken at cross-line location of 5,770 meters. Figure 5b shows the corresponding migrated image obtained by common-azimuth migration. The section is well imaged everywhere, with the exception of the bottom of the salt around in-line location of 4,000 meters. This inaccuracy in the image is likely to be caused by the common-azimuth approximation.

Figure 6 compares the results of common-azimuth migration and full source-receiver migration with 8 cross-line offsets and the application of the coplanarity condition. It shows three zooms into

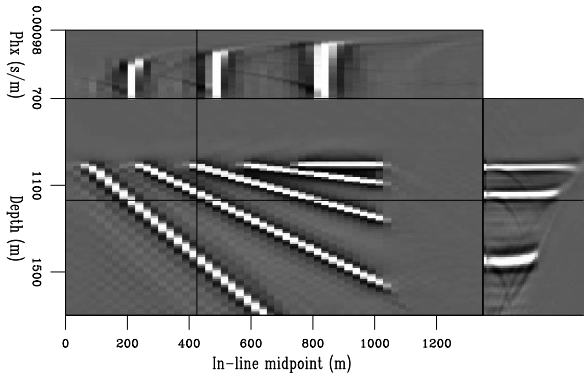

Figure 2: Subset of the results of common-azimuth migration of the synthetic data set. The front face of the cube is an in-line section through the stack. The other two faces are sections through the prestack image.

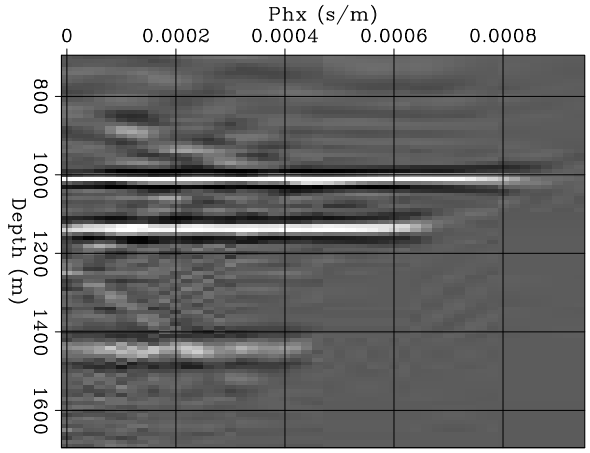

Figure 3: ADCIG extracted at the same location as the ADCIG shown in Figure 2, but from the migrated image obtained by a full source-receiver migration with $N_{y_h} = 16$.

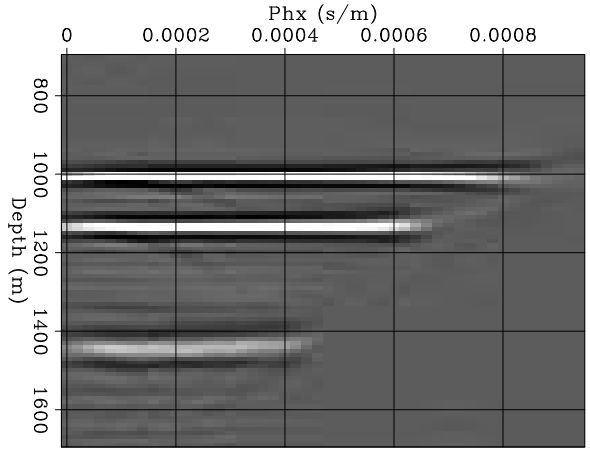

Figure 4: ADCIG extracted at the same location as the ADCIG shown in Figure 2, but from the migrated image obtained by narrow-azimuth migration with $N_{y_h} = 4$.

the area of interest. Figure 6a shows the velocity model. Figure 6b shows the image obtained by common-azimuth migration. Figure 6c shows the result of stacking the images obtained by applying the coplanarity condition on the azimuthal range defined by $|\phi| \leq 16$ degrees. Notice the improved definition of the bottom of the salt in Figure 6c compared to Figure 6b.

Similar improvements are visible in the corresponding depth slices. Figure 7 compares the slices taken at a depth of 2,600 meters. Figure 7a shows the velocity model. Figure 7b shows the image obtained by common-azimuth migration. Figure 7c shows the result of stacking the images obtained by applying the coplanarity condition on the azimuthal range defined by $|\phi| \leq 16$ degrees. Now the salt bottom boundary located between in-line locations of 4,000 and 4,500 meters is well defined. Notice that the portion of the salt boundary that is not well delineated by the image (between in-line locations of 3,000 and 3,500 meters) is not properly illuminated by the data.

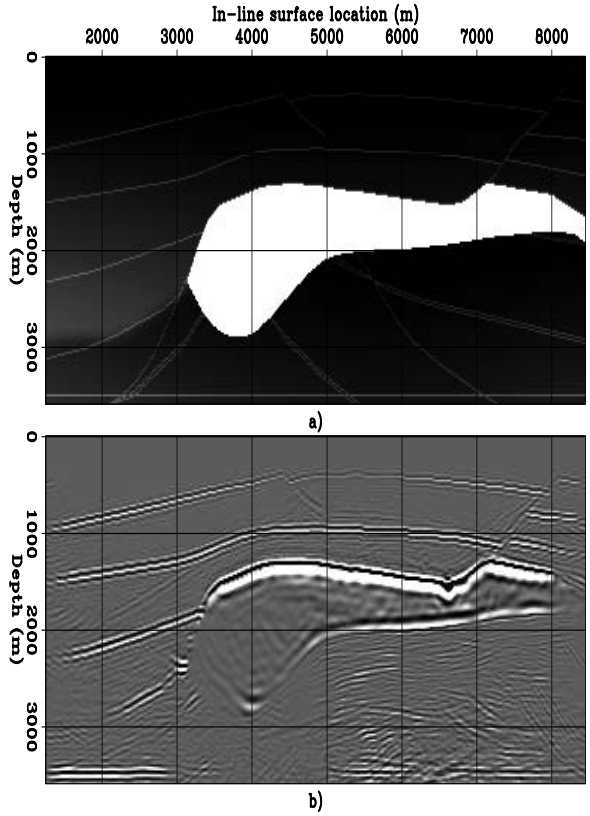

Figure 5: In-line sections (y_m =5,770 m): (a) the velocity model, (b) common-azimuth migration.

CONCLUSIONS

I presented a "narrow-azimuth" generalization of common-azimuth migration that overcomes the accuracy limitations and retains the computational efficiency of the original method. The new method is based on: 1) the definition of an "optimal" range of cross-line offset dips for the downward continuation, and 2) application of a "coplanarity" condition on the prestack image for enhancing the correctly focused events. The migration examples show that the new method has the potential of correcting the inaccuracy introduced by common-azimuth migration even in challenging situations such as the one presented by the SEG-EAGE salt data set.

ACKNOWLEDGMENTS

I would like to thank the sponsors of the Stanford Exploration Project for their financial support.

REFERENCES

Biondi, B., and Palacharla, G., 1996, 3-D prestack migration of common-azimuth data: Geophysics, **61**, no. 6, 1822–1832.

Biondi, B., Tisserant, T., and Symes, W., 2003, Wavefield-continuation angle-domain common-image gathers for migration velocity analysis: 73rd Ann. Internat. Meeting.

Biondi, B., 2002, Equivalence of source-receiver migration and shot-profile migration: Geophysics, accepted for publication.

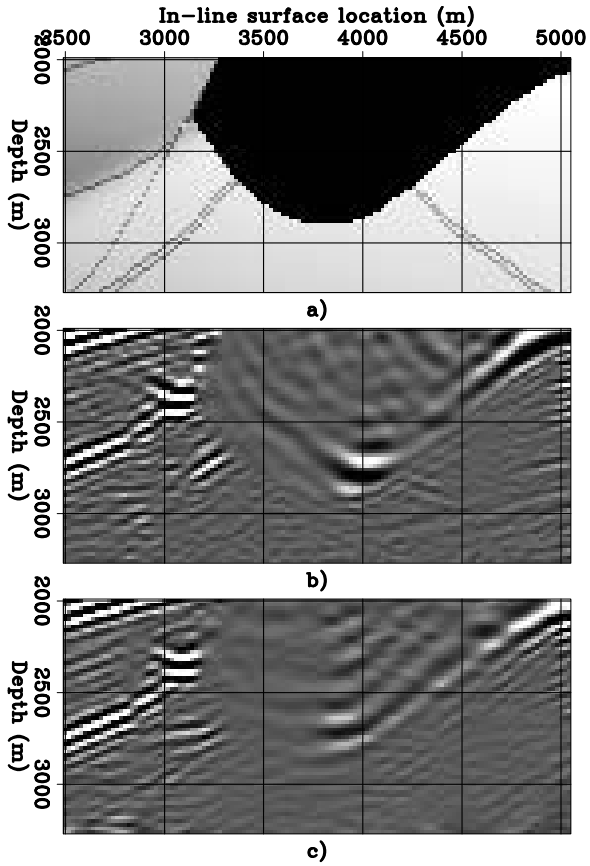

Figure 6: Zooms of the in-line sections (y_m =5,770 m): (a) the velocity model (b) common-azimuth migration, (c) full source-receiver migration with 8 cross-line offsets and the application of the coplanarity condition.

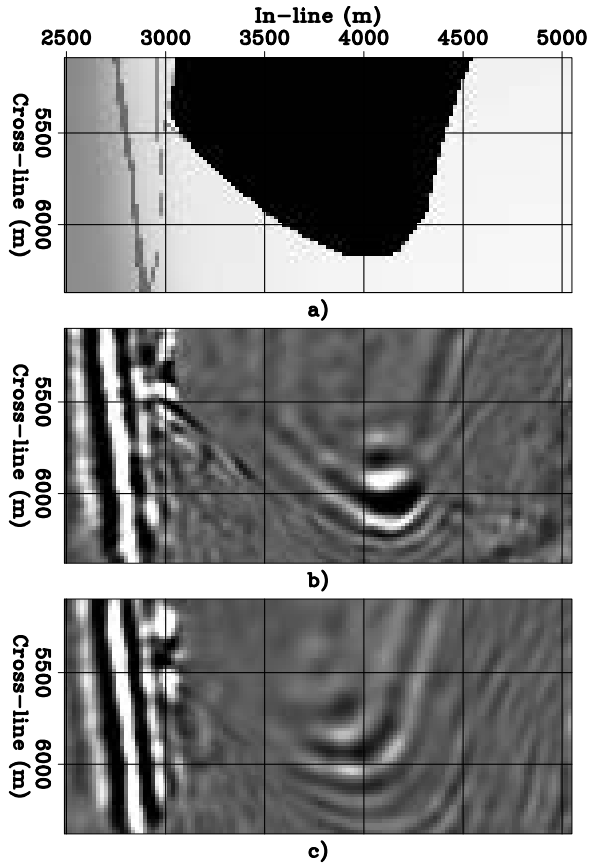

Figure 7: Zooms of the depth slices (z =2,600 m): (a) the velocity model (b) common-azimuth migration, (c) full source-receiver migration with 8 cross-line offsets and the application of the coplanarity condition.

Claerbout, J. F., 1985, Imaging the Earth's Interior: Blackwell Scientific Publications.

Clapp, R., and Biondi, B., 2000, Tau domain migration velocity analysis using angle CRP gathers and geologic constrains: 70th Ann. Internat. Mtg., Soc. of Expl. Geophys., Expanded Abstracts, 926–929.

Fliedner, M. M., Crawley, S., Bevc, D., Popovici, A. M., and Biondi, B., 2002, Velocity model building by wavefield-continuation imaging in the deepwater gulf of mexico: The Leading Edge, **21**, no. 12, 1232–1236.

Jin, S., Mosher, C., and Wu, R.-S., 2002, Offset-domain pseudo-screen prestack depth migration: Geophysics, **67**, no. 6, 1895–1902.

Le Rousseau, J., Calandra, H., and de Hoop, M., 2002, 3-D depth imaging with generalized screens: A salt body case study: CWP–**398**, `http://http://www.cwp.mines.edu/project02.html`.

Liu, W., Popovici, A., Bevc, D., and Biondi, B., 2001, 3-D migration velocity analysis for common image gathers in the reflection angle domain: 69th Ann. Internat. Meeting, Soc. of Expl. Geophys., Expanded Abstracts, 885–888.

Prucha, M., Biondi, B., and Symes, W., 1999, Angle-domain common-image gathers by wave-equation migration: 69th Ann. Internat. Meeting, Soc. Expl. Geophys., Expanded Abstracts, 824–827.

Sava, P., and Fomel, S., 2003, Angle-domain common-image gathers by wavefield continuation methods: Geophysics, accepted for publication.

Wapenaar, C. P. A., and Berkhout, A. J., 1987, Full prestack versus shot record migration: 69th Ann. Internat. Meeting, Soc. of Expl. Geophys., Expanded Abstracts, Session:S15.7.